

# Modeling of negative bias temperature instability

Tibor Grasser and Siegfried Selberherr

**Abstract**— Negative bias temperature instability is regarded as one of the most important reliability concerns of highly scaled PMOS transistors. As a consequence of the continuous downscaling of semiconductor devices this issue has become even more important over the last couple of years due to the high electric fields in the oxide and the routine incorporation of nitrogen. During negative bias temperature stress a shift in important parameters of PMOS transistors, such as the threshold voltage, subthreshold slope, and mobility is observed. Modeling efforts date back to the reaction-diffusion model proposed by Jeppson and Svensson thirty years ago which has been continuously refined since then. Although the reaction-diffusion model is able to explain many experimentally observed characteristics, some microscopic details are still not well understood. Recently, various alternative explanations have been put forward, some of them extending, some of them contradicting the standard reaction-diffusion model. We review these explanations with a special focus on modeling issues.

**Keywords**— reliability, negative bias temperature instability, modeling, simulation, hydrogen, silicon dioxide, defects, interface states, semiconductor device equations.

## 1. Introduction

After its discovery forty years ago [1, 2] negative bias temperature instability (NBTI) has again moved to the center of scientific attention as a significant reliability concern for highly scaled PMOSFETs [3–7]. This is largely due to the increased electric fields inside the gate-oxide, the presence of nitrogen, and the increased operating temperatures. During bias temperature stress which is normally introduced via a large negative voltage at the gate with drain and source remaining grounded, a shift in device parameters is observed, for instance in the threshold voltage, the subthreshold slope, and the mobility [3, 6]. In particular, the shift of the threshold voltage is often described by a simple power-law

$$\Delta V_{th}(t) = A(T, E_{ox})t^n, \quad (1)$$

with  $A$  being a coefficient which depends on temperature and the electric field. While in earlier investigations [8, 9] the exponent  $n$  in Eq. (1) was given to be in the range 0.2–0.3, newer investigations [10–12] show that  $n$  can be as small as 0.12. In particular it was found that the experimentally determined exponent is very sensitive to the measurement setup. Although this exponent is believed to be the fundamental signature of NBTI [4, 5], the values reported in literature still show a significant scatter. However, the exponent has to be determined as accurately as possible

to allow long term extrapolation of device life-times, which are commonly more than ten years, depending on the application, based on relatively short measurements obtained within a couple of days or weeks [13].

Many explanations of NBTI have been given over the years, practically all relying on the depassivation of dangling bonds at the Si/SiO<sub>2</sub> interface during stress. These dangling bonds, which are commonly known as  $P_b$  centers [14–16], are present in a considerable number at every Si/SiO<sub>2</sub> interface. During device fabrication they have to be passivated through some sort of hydrogen anneal [3], thereby eliminating the electrically active trap levels. Although the resulting  $P_bH$  bonds are very stable, at elevated temperatures and higher electric fields they can be broken, thus reactivating the electrically active trap levels. The charge stored in the  $P_b$  centers depends on the position of the Fermi-level and thus on the bias conditions. In addition, fixed positive interface charges might be created, the origin of which is attributed to H<sup>+</sup> or trapped holes.

Of particular importance in that context is the relaxation of the induced damage which is observed as soon as the stress is removed. This recovery can be quite large but the microscopic origin is not completely understood. It was found in 2003 that this effect is extremely important in the understanding of NBTI, because during measurements unintentional recovery had distorted practically all previously available measurement data [10, 12, 17].

Although a lot of progress has been made in the understanding of NBTI, a universally accepted theory is still missing. Many publications focus on refining the classic reaction-diffusion model originally proposed by Jeppson and Svensson [4, 5, 8, 9, 18, 19]. Extended versions of the reaction-diffusion model have been successfully calibrated to a wide range of measurement data reproducing a considerable number of phenomena like temperature dependent slopes via measurement artifacts, AC/DC differences, and saturation effects. However, especially the behavior in the relaxation phase is only qualitatively reproduced. This is demonstrated in Fig. 1 where the NBTI degradation during subsequent stress/relaxation cycles is shown for two different reaction-diffusion models, where good accuracy is only obtained during the first stress phase. During relaxation some apparent saturation is often observed which is not well reproduced. Also, if stress is applied again, the accuracy of the results predicted by the reaction-diffusion model decreases (also see for instance fits to measurements in [4, 20]).

Recently a variety of other explanations for bias temperature instability have been put forward, using for instance

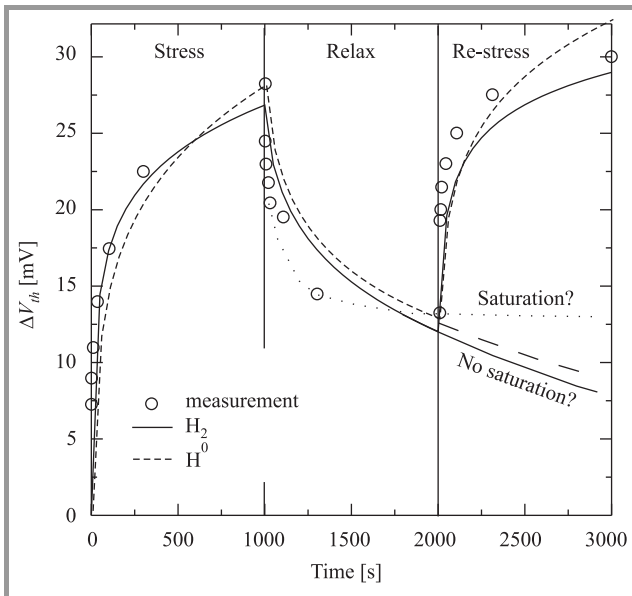


**Fig. 1.** NBTI degradation during subsequent stress/relaxation cycles. Although good accuracy can be obtained during the first stress phase, the fit is only qualitative and considerably poorer during the second stress phase. Shown are the results of the standard reaction-diffusion model with  $H^0$  and  $H_2$  kinetics together with measurement data from [4].

dispersive transport of the hydrogen species released from the dangling bond [21–23], creation of hole traps [6], a broad distribution of dissociation rates at the interface [6, 24, 25] and interactions with hydrogen from the inversion layer [26]. Some of these extended/alternative models rely on a different microscopic picture, sometimes augmenting – but not always compatible with – the standard reaction-diffusion model.

For modeling NBTI it is often tried to identify a *single dominant* mechanism which determines the asymptotic behavior of NBTI. With various simplifying assumptions a closed form expression for the  $V_{th}$  shift over time is sought. As of yet, however, no universally accepted dominant mechanism could be isolated. One can conclude that several mechanisms are at work, each dominant over the other ones in certain devices (nitrided oxides [27], high- $k$  [28], ultra-thin oxides [5] compared to power devices with thicker oxides [29]) under certain processing or stressing conditions.

## 2. Experimental issues

Experimental determination of NBTI induced  $V_{th}$  shifts suffers from some fundamental difficulties. To determine the  $V_{th}$  shift the stressing voltage on the gate has to be removed, and in addition to  $I_D - V_G$  sweeps, capacitance-voltage and charge pumping measurements are often conducted to separate the potential contribution of interface and oxide charges. Unfortunately, with the stressing voltage removed from the gate, the inverse reaction of the depassivation process is favored, resulting in an extremely fast ( $< 1$  ms or even  $1 \mu\text{s}$ ) relaxation [6, 10–12]. This relax-

ation seems to depend on the processing, stressing, and relaxation conditions. While most groups report only partial recovery [6], 100% recovery has also been reported [11] in addition to a contradicting dependence of the recovery rate on the applied gate bias [6, 30–32].

To avoid any interference of this recovery process with the measured data, it has been suggested to measure the drift *without* interruption of the stress condition [6, 17]. One variant just monitors the change in the drain current in the linear regime which is then traced back to a threshold voltage shift via the initial  $I_D - V_G$  characteristic [19]. Other variants have been proposed where small variations to the bias conditions can be added allowing the determination of  $\Delta I_{d,lin}$  and  $\Delta g_m$ . A drawback of these on-the-fly measurements is that they measure the change in the drain current in the linear regime, where the occupancy of the traps might be different from the one observed during real operating conditions.

Although unintentional measurement delay is detrimental for life-time extrapolation, valuable information about the relaxation physics can be obtained by studying the influence of the measurement delay [10, 19, 30, 33] on the result. Since most of the relaxation occurs within the first milliseconds, extremely fast measurement techniques have been developed [33] which allow to study delays as short as  $1 \mu\text{s}$ .

## 3. Physical mechanisms

Although the reaction-diffusion model [5, 8, 18] is often successful in describing measurements, knowledge of the underlying microscopic physics is still vague [21–23]. In the following, the most important processes likely to occur during negative bias temperature stress are summarized. They comprise the depassivation and annealing of interface states and the behavior of the released hydrogen inside the surrounding materials. In addition to, or even instead of the chemical reactions underlying the reaction-diffusion model, various other reactions may occur. These reactions are shown schematically in Fig. 2 and explained in more detail in the following.

### 3.1. Hydrogen in semiconductor devices

Most degradation mechanisms reported in the context of NBTI are closely linked to the existence of hydrogen in  $\text{SiO}_2$ , Si, and p-Si. Hydrogen in these materials is amphoteric and occurs for instance as  $H^0$ ,  $H^+$ ,  $H^-$ , and  $H_2$ . Due to its negative-U character  $H^0$  is unstable at room temperature [34] and depending on the position of the Fermi-level turns into  $H^+$  or  $H^-$ , or dimerizes within a fraction of a second [15]. However, atomic hydrogen occurs as a transient quantity during various reactions. In particular, release of atomic hydrogen is assumed in the reaction-diffusion model which then quickly dimerizes into  $H_2$ . However, both  $H^0$  and  $H_2$  are extremely fast diffusers and atomic hydrogen is released from spatially

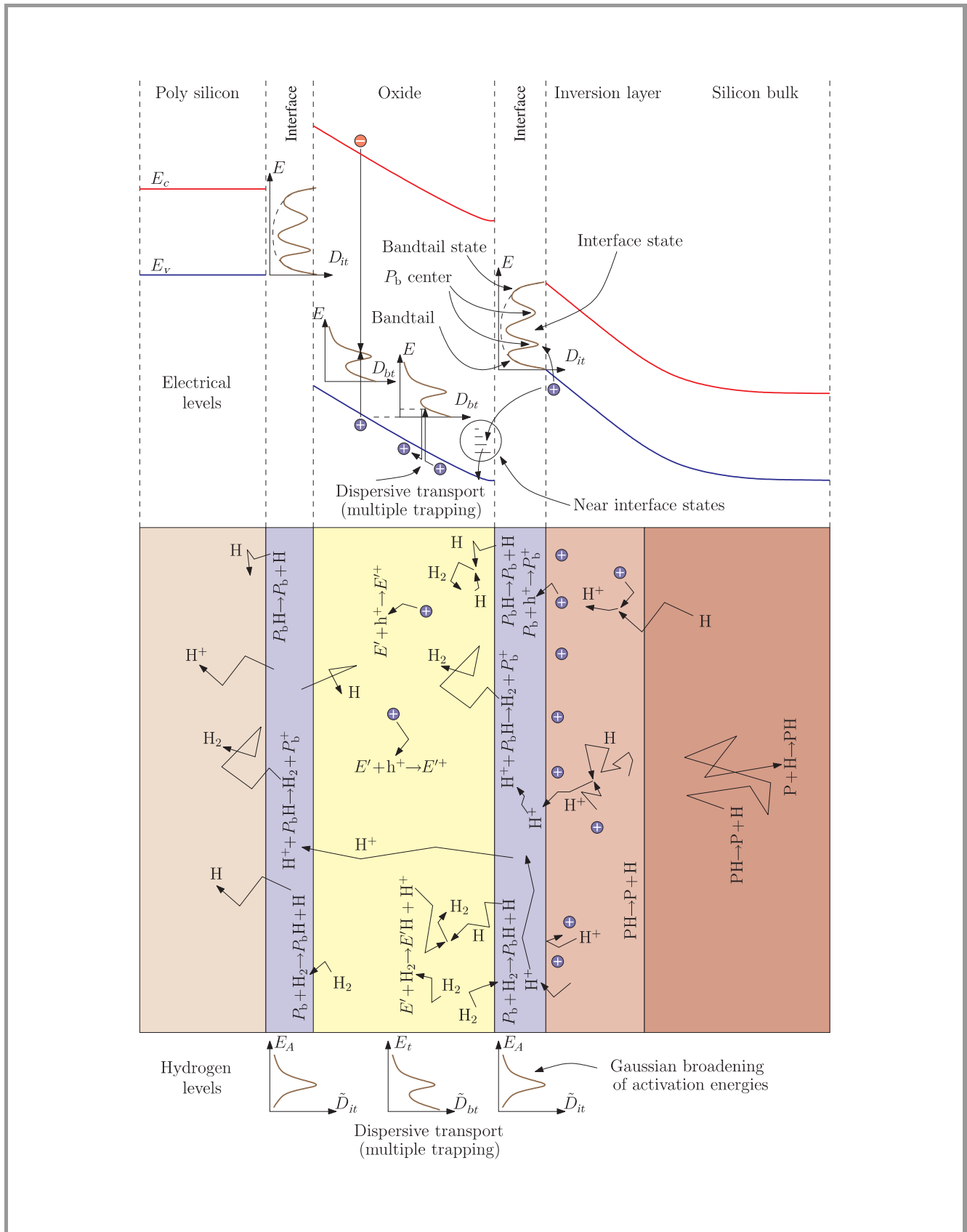


Fig. 2. Various processes reported in the context of NBTI.

separated dangling bonds which might reduce the dimerization rate. Therefore, it is not straightforward to decide whether dimerization occurs first, whether atomic hydrogen leaves the oxide before being able to dimerize, or whether atomic hydrogen turns into  $H^+$ , its energetically most favorable state [34].

Another interesting issue stems from the fact that in semiconductor devices hydrogen is present in large amounts. Hydrogen is either unintentionally introduced during the various processing steps or intentionally during the required hydrogen anneals to passivate defects at the Si/SiO<sub>2</sub> interface and dangling bonds in the p-Si-gate. For instance, [35] reported a background H concentration of  $10^{19} \text{ cm}^{-3}$  in p-Si. With a “free” hydrogen concentration as large as that, the reverse reaction in the reaction-diffusion model would always be very large, and consequently a very small time exponent would be expected, in contradiction to measurement results. Thus, one needs to assume that most hydrogen is trapped, possibly on shallow bond-center sites or in deep traps formed by dangling bonds, for instance at grain boundaries in p-Si. Trapped hydrogen, however, is not part of the standard reaction-diffusion picture.

Based on first-principle studies [26] it was proposed that the release of the proton is energetically preferable. However, dimerization of  $H^+$  is unlikely due to electrostatic repulsion. In addition, depending on the process conditions,  $H^+$  can be either extremely stable or highly reactive [36]. A proper understanding of the various hydrogen species in SiO<sub>2</sub>, Si, p-Si, is thus essential [34] to justify the microscopic picture underlying the reaction-diffusion or alternative models. Matters become further complicated due to the various interactions of hydrogen species with dopants [37] and some additional effects occurring for instance in nitrided oxides [38, 39].

### 3.2. Dispersive transport

Although the reaction-diffusion model relies on conventional diffusive transport, dispersive transport equations are often used to describe the motion of the hydrogen species in dielectrics and amorphous materials [40–44]. In particular, the type of transport seems to depend on the hydrogen concentration, being diffusive for hydrogen concentrations larger than the trap-density and dispersive otherwise. In the dispersive case the traveling particle packet slows down [45] due to the trapping in states with a broad distribution of release times. As a consequence, the shape of the particle packet becomes non-Gaussian. As a measure of dispersivity one may look at the ratio of the mean and the standard deviation of the particle packet [46]. While for the Gaussian packet this ratio increases with time, it stays roughly constant in the dispersive case, indicating an anomalous spreading of the particle packet. A typical impulse response of the average flux of a dispersive system in comparison to a diffusive system is shown in Fig. 3. Characteristic for dispersive transport is the rapid decline in the beginning (where particles start to fill the traps), followed by a broad

shoulder which eventually develops a long tail (note the logarithmic time scale). The response of a diffusive system, on the other hand, vanishes after a transit time of approximately  $L^2/D$ , where  $L$  is the sample thickness and  $D$  the diffusion coefficient.

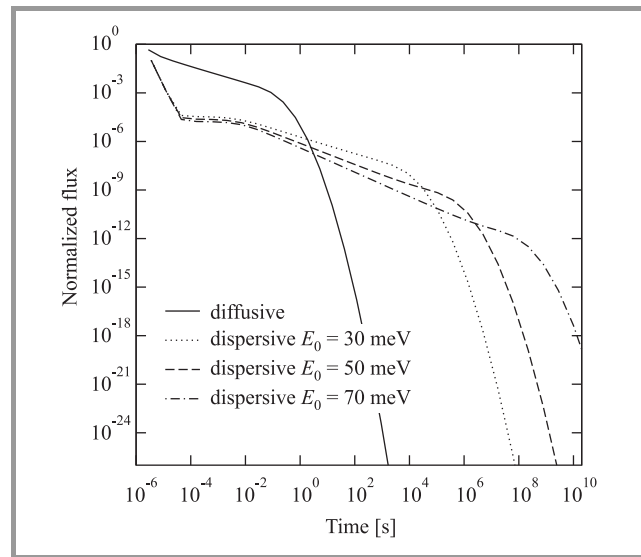


**Fig. 3.** Impulse response of a diffusion system in comparison to a dispersive system for various characteristic trap energies. Typical for dispersive transport is the rapid decline in the beginning, the shoulder, followed by a long tail.

Dispersive transport models were first applied to describe the movement of holes in amorphous materials [41] and  $H^+$  after irradiation damage [44]. While the first studies were based on the continuous time random walk (CTRW) theory developed by Scher and Montroll [40, 41, 44], multiple trapping (MT) models were proposed soon afterwards [42, 43, 45]. Both models exhibit similar features [47–49] and simplified versions were used to describe NBTI [21–23]. The basic quantity in the CTRW approach is the hopping time distribution which gives the hopping probability from one state to the next. As such, this approach is well suited for Monte-Carlo techniques but analytic solutions for the CTRW equations cannot be given for the general case. Approximate solutions have been commonly sought using the inverse Laplace transformation of the system’s Green’s function through suitable trial functions, either analytically or numerically [44, 46, 50, 51].

The MT model, on the other hand, uses partial differential equations compatible to the equations conventionally used in process and device simulation and are therefore – in our opinion – more suitable for the inclusion into a numerical simulator. In the MT model the species  $X(\mathbf{x}, t)$  consists of free (conducting) particles  $X_c(\mathbf{x}, t)$  and particles residing on various trap levels  $E_t$ . The energy density of those trapped particles is given by  $\rho(\mathbf{x}, E_t, t)$  and the total concentration is calculated as

$$X(\mathbf{x}, t) = X_c(\mathbf{x}, t) + \int \rho(\mathbf{x}, E_t, t) dE_t. \quad (2)$$

The continuity equation for the total concentration of the species  $X$  reads

$$\frac{\partial X(\mathbf{x}, t)}{\partial t} = -\nabla \cdot \mathbf{F}_{Xc}(\mathbf{x}, t), \quad (3)$$

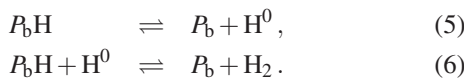
where the flux is only determined by particles in the conduction states. At each trap level a balance equation accounts for the newly trapped particles versus the released ones. The release rate is proportional to the trapped charge on that level, assuming appropriate space in the extended states:

$$\frac{\partial \rho(\mathbf{x}, E_t, t)}{\partial t} = c(E_t)X_c(\mathbf{x}, t)(g(E_t) - \rho(\mathbf{x}, E_t, t)) - r(E_t)\rho(\mathbf{x}, E_t, t). \quad (4)$$

Here,  $c(E_t)$  and  $r(E_t)$  are the energy-dependent capture and release rates, respectively, and  $g(E_t)$  is the trap density of states, where commonly an exponential distribution is assumed. In that context some caution is in order: although hydrogen motion can be phenomenologically described by equations similar to electron transport in semiconductors there are some fundamental differences [52]. First, the configuration of the host material can permanently change as a consequence of hydrogen motion. Second, transport does probably not occur near a mobility edge but rather through hopping from individual shallow states. In addition, hydrogen clusters, known as platelets [37], may form making the application of the trap occupancy concept more involved. Nevertheless, relatively simple models based on two trap levels (shallow and deep) have been successfully used to describe hydrogen motion in a wide range of materials.

### 3.3. Interface states

The central mechanism in NBT degradation is the dissociation of  $P_bH$  bonds located at the Si/SiO<sub>2</sub> interface, most possibly through reactions like



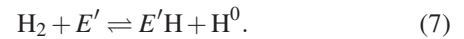
The forward reaction in Eq. (5) is commonly assumed to be the dominant dissociation mechanism. Although the reverse reaction, which is responsible for the passivation through atomic hydrogen, is highly effective, its total impact is normally insignificant [53] due to the low concentration of  $H^0$ . However, for the special case of radiation environments, where large quantities of atomic hydrogen are generated in the oxide, and for hot carrier effects it becomes important [54, 55]. In particular, combined NBTI/hot carrier/irradiation stress would be a good probe for the validity of a general model.

Equations (5) and (6) also explain the dual behavior of hydrogen as being able to passivate and to depassivate dangling bonds. The reverse reaction through  $H_2$  without preliminary cracking [53] is sometimes assumed to be the dominant reaction in the case of NBT stress [56]. Activation energies for the first-order reaction given through

Eq. (6) were traditionally estimated to be around 1.6 eV. Recent work has shown that although the first-order kinetics can be confirmed, a Gaussian distribution of activation energies around 1.5 eV with a standard deviation of 0.15 eV has to be considered [24, 57].

### 3.4. Oxide defects

Another interesting issue is the creation or modification of defects by diffusing hydrogen. Although for ultra-thin oxides the influence of oxide traps on NBTI is controversial [5, 6], for thick oxides these defects seem to be important [29]. Some investigations report that roughly the same number of positive fixed charges as depassivated  $P_b$  centers are created [58], while others attribute NBTI induced  $V_{th}$  shifts totally to depassivated  $P_b$  centers [5], provided proper stressing conditions are chosen ( $E_{ox} < E_{crit}$ ). Most positive charges are located close to the interface and have been identified as  $E'$  centers (thermal oxide hole traps) [15].  $E'$  centers have been reported to dominate oxide hole trapping with their density being strongly process dependent [15]. It has been shown that  $E'$  centers react rapidly with  $H_2$ , even at room temperature, turning them into hydrogen complexed  $E'$  centers ( $E'H$ ) according to [53]



In addition, trapping of  $H^0$  has been reported [59]



Of particular interest in the case of NBTI is the annealing of  $E'$  centers through  $H_2$ , which was reported to bring up roughly the same amount of  $P_b$  centers [15], possibly through the following reaction, with  $H_2$  formally being a catalyst



The atomic hydrogen released in the various reactions is commonly assumed to either quickly dimerize into  $H_2$  and diffuse towards the poly gate [4, 5], assuming classical diffusion, or to move dispersively as  $H^+$  [21, 22].

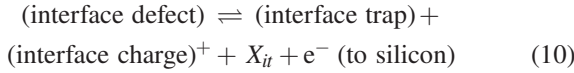
Hydrogen motion in the silicon bulk is normally neglected. This might be justified in the case of  $H_2$  based models by the large diffusion barrier found in theoretical studies [60], or in the case of  $H^+$  by the negative bias driving the protons towards the gate. Provided that the breaking of PH bonds in the Si bulk is an important source of  $H^0$  and  $H^+$  [26], transport in Si must be included in a rigorous model.

## 4. Models

Using a combination of some selected mechanisms summarized above a considerable number of different NBTI models has been proposed. Of particular interest in that case is the fact that although these models rely on different microscopic contexts, they all seem to reproduce the measurement data published alongside them.

#### 4.1. The reaction-diffusion model

The reaction-diffusion model dates back to the work of Jeppson and Svensson [8]. They assumed an electrochemical reaction of the form



at the interface where the hydrogen species created at the interface ( $X_{it}(t) = X(0, t)$ ) is assumed to diffuse away into the oxide. The exact chemical composition of the diffusing species is still under debate, although strong arguments for  $H_2$  have been presented [4, 5, 12, 19]. In the reaction-diffusion model  $H_2$  results in a characteristic time exponent of  $1/6$ , closest to experimentally observed values. Atomic hydrogen, on the other hand, with an exponent of  $1/4$  was favored in older publications, consistent with measurement data available at that time.  $H^+$ , previously neglected, because it results in an exponent of  $1/2$ , recently entered the scene [21–23] because dispersive transport models seem to allow to adjust the slope to smaller values. As of yet, however, the scatter in the experimentally observed time exponents is still too large to settle for a single diffusing species and one explanation could be the simultaneous creation, diffusion, and interaction of several hydrogen species [61]. The kinetic equation describing the interface reaction is [9, 56, 62]

$$\frac{\partial N_{it}}{\partial t} = k_f(N_0 - N_{it}) - k_r N_{it} X_{it}^{1/a}, \quad (11)$$

where  $N_{it}$  is the surface state concentration,  $N_0$  the initial concentration of passivated interface defects,  $k_f$  and  $k_r$  the field and temperature dependent rate coefficients, while  $a$  is the kinetic exponent (1 for  $H^0$  and  $H^+$ , and 2 for  $H_2$ ). Note that the same equation is obtained assuming instantaneous dimerization of  $H^0$  into  $H_2$  [56].

Transport of the species  $X$  away from the interface is assumed to be controlled by conventional drift-diffusion

$$\frac{\partial X}{\partial t} = -\nabla \cdot \mathbf{F}_X, \quad (12)$$

$$\mathbf{F}_X = -D_X \nabla X + Z_X X \mu_X \mathbf{E}. \quad (13)$$

Here,  $D_X$ ,  $\mu_X$ , and  $Z_X$  are the diffusion coefficient, the mobility and the charge state of species  $X$  in the medium. Diffusivity and mobility are assumed to be independent of the electric field and to be related via the Einstein relation [61]:

$$\mu_X = \frac{q D_X}{k_B T_L} = \frac{D_X}{V_T}. \quad (14)$$

Note that this is not the case for a dispersive medium where strongly different temperature dependencies can be observed in the equilibrium regime. At the boundary we have to consider the influx of the newly created species

$$a \frac{\partial N_{it}}{\partial t} = \mathbf{F}_X \cdot \mathbf{n}. \quad (15)$$

For the general case, Eqs. (11)–(15) can be solved numerically. However, for some special cases analytical approximations can be given [18, 56, 63] which are helpful for the understanding of the basic kinetics. One finds different phases, starting from the reaction dominated regime with slope  $n = 1$ , where the reverse rate is negligible due to the lack of available  $X$ , a transition regime with slope  $n = 0$ , the quasi-equilibrium regime with  $\partial N_{it}/\partial t \approx 0$ , which is the dominant regime and displays the characteristic time exponent depending on the created species, and a saturation

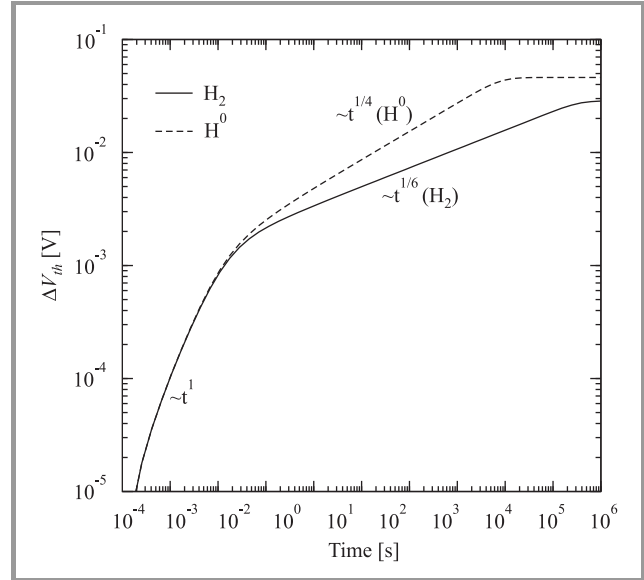


**Fig. 4.** The three most important phases in the reaction-diffusion model. Shown are the results for  $H^0$  and  $H_2$  kinetics. The time exponent  $n = 1$  is the signature of the reaction limited phase while  $n = 1/4$  and  $n = 1/6$  result from the diffusion limited phase.

regime. These phases are shown in Fig. 4 for  $H^0$  and  $H_2$  kinetics. Of particular interest is the result for  $\partial N_{it}/\partial t \approx 0$ , which is the one normally measured during NBTI stress. For atomic hydrogen one obtains

$$N_{it}(t) = \sqrt{\frac{k_f N_0}{2k_r}} (D_X t)^{1/4}, \quad (16)$$

while molecular hydrogen results in

$$N_{it}(t) = \left( \frac{k_f N_0}{2k_r} \right)^{2/3} (D_X t)^{1/6} \quad (17)$$

and the hydrogen proton gives

$$N_{it}(t) = \sqrt{\frac{k_f N_0}{k_r}} (\mu_X E_{ox} t)^{1/2}. \quad (18)$$

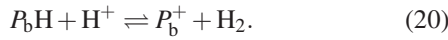
Of course, the characteristic exponents for each species given above rely on the validity of the reaction-diffusion model and different exponents can be envisaged using an alternative model [21–23].

From the calculated interface state density  $N_{it}$  the threshold voltage shift has to be determined. This is performed by assuming that all traps are positively charged, an assumption fulfilled during strong negative bias where the Fermi-level is close to the valence band edge. In addition, the generated oxide charges are often neglected and we obtain

$$\Delta V_{th} = -\frac{\Delta Q_{it}(E_F) + \Delta Q_{ot}}{C_{ox}} \approx -\frac{q\Delta N_{it}}{C_{ox}}. \quad (19)$$

Due to the increased Coulomb scattering at the interfacial layer caused by charged interface states the carrier mobility decreases [64, 65]. However, for the analysis of NBTI, any potential mobility degradation has so far been neglected [20].

Based on first-principles calculations, the dissociation of  $P_bH$  through  $H^+$  has been suggested as the dominant reaction [26], thereby replacing reaction Eq. (5):



The required  $H^+$  is provided through broken PH bonds in the silicon bulk inversion layer. After overcoming the migration barrier at the interface, some  $H^+$  diffuses along the interface before depassivating  $P_b$  centers. Alternatively, some  $H^+$  can surmount the energy barrier towards the  $SiO_2$  where they quickly drift to the gate due to the strong electric field.

#### 4.2. Models assuming dispersive transport

Based on simplified solutions for the MT problem NBTI models have been developed [22, 30]. For the extremely non-equilibrium case Arkhipov and Rudenko derived [43]

$$\frac{X(\mathbf{x}, t) - X_0(\mathbf{x})}{\tau(t)} = -\nabla \cdot \mathbf{F}_X(\mathbf{x}, t) \quad (21)$$

which describes the broadening of the initial distribution  $X_0(\mathbf{x})$ . Here the flux is given through an “effective” flux of the total concentration of the species  $X$  rather than the concentration in the conduction states. Note, that there is no time derivative in Eq. (21) and the dynamics of the system have been incorporated into  $\tau(t)$  which directly depends on the density of states. Starting from Eq. (21), assuming an exponential density of states with a characteristic energy  $E_0$  and density  $N_t$ , and  $\partial N_{it}/\partial t \approx 0$ , Kaczer *et al.* derived [22]

$$N_{it}(t) = \sqrt{\frac{k_f N_0}{k_r}} \left( \frac{D_X N_c}{v_0 N_t} \right)^{1/4} (v_0 t)^{\alpha/4}, \quad (22)$$

with  $\alpha = k_B T_L / E_0$ . Interestingly, the time exponent is given here through  $n = \alpha/4$  and thus explicitly depends on temperature, a phenomenon sometimes observed experimentally [4, 6, 22], but also ascribed to a measurement artifact [66]. Note that  $\alpha$  is in the range  $0 \leq \alpha \leq 1$  with  $\alpha = 1$  being the diffusive limit.

Using simple arguments from statistical mechanics in addition to the assumption of dispersive transport of  $H^+$  inside

the oxide, Zafar [23] derived a stretched-exponential relation for the threshold voltage shift as

$$\frac{\Delta V_{th}(t)}{\Delta V_{th, \max}} = 1 - \exp\left(-\left(\frac{t}{\tau}\right)^{-\alpha}\right). \quad (23)$$

Here,  $\Delta V_{th, \max}$  gives the maximum threshold voltage shift,  $\tau$  is the characteristic time constant, and  $\alpha$  the dispersion parameter. At early times, the above equation assumes a similar form as the expression derived by Kaczer *et al.* [22].

#### 4.3. Reaction-limited models

Houssa *et al.* [67] base their NBTI model for nitrided oxides on the assumption that the dissociation rate is determined by electron and hole tunneling currents. Employing a Gaussian distribution of activation energies, interface traps are generated by releasing a proton which is later trapped inside the oxide forming oxide charges. With these assumptions the contributions due to electrons and holes can be separated, indicating a dominance of hole induced damage at operating voltages. Consequently, if for accelerated tests higher voltage levels are used, the electron contribution begins to dominate which makes long-term extrapolation difficult.

This Gaussian distribution of activation energies was also used as the main ingredient in the reaction-limited model of Huard *et al.* [68] who assume an energy-dependent distribution of the dissociation activation energy

$$g(E_d, \sigma) = \frac{1}{\sigma} \frac{\exp\left(\frac{E_{dm} - E_d}{\sigma}\right)}{\left(1 + \exp\left(\frac{E_{dm} - E_d}{\sigma}\right)\right)^2}. \quad (24)$$

In the above equation the median dissociation energy  $E_{dm}$  was assumed to depend on the oxide electric field in order to accommodate the reported field dependence. The threshold voltage shift was then derived as

$$\frac{\Delta V_{th}}{\Delta V_{th, \max}} = \frac{1}{1 + \left(\frac{t}{\tau}\right)^{-\alpha}} \quad (25)$$

with  $\tau = \tau_0 \exp(E_d(E_{ox})/k_B T_L)$  and  $\alpha = k_B T_L / \sigma$ . Again, as with the dispersive transport model, a temperature dependent slope is obtained.

## 5. Other modeling issues

In addition to the issues raised above, some further considerations are required in order to develop a comprehensive model. They are summarized in the following.

#### 5.1. Boundary conditions

An important issue is the behavior of the hydrogen species when they encounter the  $SiO_2/p$ -Si interface. Commonly, simplified boundary conditions to the diffusion equation

are assumed, either perfect reflection [9, 69], perfect absorber [9], or perfect transmitter [4] (no trapping). However, for a rigorous treatment one might have to consider the energy barriers [60], the creation and passivation of  $P_b$  centers [28], and re-emission of hydrogen on the p-Si side, analogous to the Si/SiO<sub>2</sub> interface and models used in process-simulation [70].

### 5.2. Geometry dependence

Negative bias temperature instability is commonly assumed to be a one-dimensional process [71], which is in agreement with many reported results, while only the closely related damage caused by hot-carrier injection is acknowledged to require a two-dimensional treatment of the diffusion equation. Even if all processes leading to NBTI were one-dimensional, inhomogeneous doping profiles [72], variable oxide thicknesses such as found in high-voltage devices, inhomogeneities observed around shallow trench isolations, or inhomogeneous stress conditions ( $V_{DS} \neq 0$ ) [72] require a two- or even three-dimensional description of the problem. Even for homogeneous stress ( $V_{DS} = 0$ ) a gate length dependence is occasionally reported [3]. For highly scaled MOSFETs or MOSFETs with a narrow channel the geometry influences the diffusion of the released hydrogen species, an effect contained in the classic reaction-diffusion model [73]. Other explanations are based on diffusion of H<sup>+</sup> along the interface as observed experimentally [74] and confirmed theoretically [36].

### 5.3. Coupling to semiconductor equations

A commonly neglected issue in NBTI modeling is the coupling of the “hydrogen equations” to the semiconductor device equations for current transport. In particular, the dynamic creation and annihilation of  $P_b$  and  $E'$  centers influences the electric field distribution and thus the reaction rates and the transport properties. This issue is of particular importance when annealing during measurements [17] is to be understood. Some issues need to be resolved when such a coupling is attempted. First, the charge trapped in the amphoteric  $P_b$  centers depends on the position of the Fermi-level and thus on the bias conditions. To model this effect, the density of  $P_b$  centers created needs to be coupled to the electrically active interface trap density-of-states  $D_{it}(\mathcal{E})$  in a surface recombination process [75]. A lot of information on  $D_{it}$  is available and it is known that in addition to the band-tail states  $P_b$  centers introduce two distinct peaks in the Si band gap [14, 55]. The shape of these peaks has been described using Fermi functions [13] where the two peak values evolve differently in time with each width staying roughly constant [15, 55]. Regarding the contribution of trapped holes in the oxide, precise statements on where exactly these charges are located are important to properly model the shape of the band-edges in SiO<sub>2</sub>, which directly influence the oxide field and thus charge carrier transport and tunneling rates.

A specific coupling issue concerns the influence of holes which are commonly assumed to be “available”. The dissociation rate in Eq. (5) is often assumed to depend on the concentration of the inversion layer holes, a quantity not directly available in NBTI models. Here, a rigorous coupled solution should provide better estimates. Although the importance of holes in this process is widely acknowledged, the mechanisms have not yet been evaluated rigorously and it is not clear in which way they influence the forward rate. Furthermore, electrons and holes might be required to properly account for charging and discharging of oxide and near-interface defects.

## 6. Conclusions

Although significant progress regarding the understanding of NBTI has been made in the last decade, and the reaction-diffusion model gives good qualitative agreement with many measurements, various microscopic details are still unclear. Among those are the oxide charges created during stress, the nature and transport mechanism of the created species, and the relaxation behavior. Many more consistent sets of experiments are required to aid the development and evaluation of more detailed models. Thereby the relative importance and the complex interplay between the various processes reported could be clarified.

## References

- [1] A. Goetzberger and H. E. Nigh, “Surface charge after annealing of Al-SiO<sub>2</sub>-Si structures under bias”, *Proc. IEEE*, vol. 54, no. 10, pp. 1454–1454, 1966.
- [2] E. Deal, M. Sklar, A. S. Grove, and E. H. Snow, “Characteristics of the surface-state charge (Q<sub>ss</sub>) of thermally oxidized silicon”, *J. Electrochem. Soc.*, vol. 114, no. 3, p. 266, 1967.
- [3] D. K. Schroder and J. A. Babcock, “Negative bias temperature instability: road to cross in deep submicron silicon semiconductor manufacturing”, *J. Appl. Phys.*, vol. 94, no. 1, pp. 1–18, 2003.
- [4] M. A. Alam and S. Mahapatra, “A comprehensive model of PMOS NBTI degradation”, *Microelectron. Reliab.*, vol. 45, no. 1, pp. 71–81, 2005.
- [5] S. Mahapatra, M. A. Alam, P. B. Kumar, T. R. Dalei, D. Varghese, and D. Saha, “Negative bias temperature instability in CMOS devices”, *Microelectron. Eng.*, vol. 80, no. suppl., pp. 114–121, 2005.
- [6] V. Huard, M. Denais, and C. Parthasarathy, “NBTI degradation: from physical mechanisms to modelling”, *Microelectron. Reliab.*, vol. 46, no. 1, pp. 1–23, 2006.
- [7] J. H. Stathis and S. Zafar, “The negative bias temperature instability in MOS devices: a review”, *Microelectron. Reliab.*, vol. 46, no. 2–4, pp. 270–286, 2006.
- [8] K. O. Jeppson and C. M. Svensson, “Negative bias stress of MOS devices at high electric fields and degradation of MNOS devices”, *J. Appl. Phys.*, vol. 48, no. 5, pp. 2004–2014, 1977.
- [9] S. Ogawa and N. Shiono, “Generalized diffusion-reaction model for the low-field charge build up instability at the Si/SiO<sub>2</sub> interface”, *Phys. Rev. B*, vol. 51, no. 7, pp. 4218–4230, 1995.
- [10] M. Ershov, R. Lindley, S. Saxena, A. Shibkov, S. Minehane, J. Babcock, S. Winters, H. Karbasi, T. Yamashita, P. Clifton, and M. Redford, “Transient effects and characterization methodology of negative bias temperature instability in PMOS transistors”, in *Proc. Int. Rel. Phys. Symp.*, Dallas, USA, 2003, pp. 606–607.



- [11] S. Rangan, N. Mielke, and E. C. C. Yeh, "Universal recovery behavior of negative bias temperature instability", in *Proc. Int. Electron Dev. Meet.*, Washington, USA, 2003, pp. 341–344.
- [12] D. Varghese, D. Saha, S. Mahapatra, K. Ahmed, F. Nouri, and M. Alam, "On the dispersive versus arrhenius temperature activation of NBTI time evolution in plasma nitrided gate oxides: measurements, theory, and implications", in *Proc. Int. Electron Dev. Meet.*, Washington, USA, 2005, pp. 1–4.
- [13] A. Haggag, W. McMahon, K. Hess, K. Cheng, J. Lee, and J. Lyding, "High-performance chip reliability from short-time-tests", in *Proc. Int. Rel. Phys. Symp.*, Orlando, USA, 2001, pp. 271–279.
- [14] E. H. Poindexter, G. J. Gerardi, M.-E. Rueckel, P. J. Caplan, N. M. Johnson, and D. K. Biegelsen, "Electronic traps and  $P_b$  centers at the Si/SiO<sub>2</sub> interface: band-gap energy distribution", *J. Appl. Phys.*, vol. 56, no. 10, pp. 2844–2849, 1984.
- [15] P. M. Lenahan and J. F. Conley Jr., "What can electron paramagnetic resonance tell us about the Si/SiO<sub>2</sub> system?", *J. Vac. Sci. Technol. B*, vol. 16, no. 4, pp. 2134–2153, 1998.
- [16] J. P. Campbell, P. M. Lenahan, A. T. Krishnan, and S. Krishnan, "Direct observation of the structure of defect centers involved in the negative bias temperature instability", *Appl. Phys. Lett.*, vol. 87, no. 20, pp. 1–3, 2005.
- [17] M. Denais, A. Bravaix, V. Huard, C. Parthasarathy, G. Ribes, F. Perrier, Y. Rey-Tauriac, and N. Revil, "On-the-fly characterization of NBTI in ultra-thin gate oxide PMOSFET's", in *Proc. Int. Electron Dev. Meet.*, San Francisco, USA, 2004, pp. 109–112.
- [18] M. A. Alam, "A critical examination of the mechanics of dynamic NBTI for PMOSFETs", in *Proc. Int. Electron Dev. Meet.*, Washington, USA, 2003, pp. 345–348.
- [19] A. T. Krishnan, C. Chancellor, S. Chakravarthi, P. E. Nicollian, V. Reddy, A. Varghese, R. B. Khamankar, and S. Krishnan, "Material dependence of hydrogen diffusion: implications for NBTI degradation", in *Proc. Int. Electron Dev. Meet.*, Washington, USA, 2005, pp. 688–691.
- [20] A. T. Krishnan, V. Reddy, S. Chakravarthi, J. Rodriguez, S. John, and S. Krishnan, "NBTI impact on transistor and circuit: models, mechanisms and scaling effects", in *Proc. Int. Electron Dev. Meet.*, Washington, USA, 2003, pp. 14.5.1–14.5.4.
- [21] M. Houssa, M. Aoulaiche, S. De Gendt, G. Groeseneken, M. M. Heyns, and A. Stesmans, "Reaction-dispersive proton transport model for negative bias temperature instabilities", *Appl. Phys. Lett.*, vol. 86, no. 9, pp. 1–3, 2005.
- [22] B. Kaczer, V. Arkhipov, R. Degraeve, N. Collaert, G. Groeseneken, and M. Goodwin, "Temperature dependence of the negative bias temperature instability in the framework of dispersive transport", *Appl. Phys. Lett.*, vol. 86, no. 14, pp. 1–3, 2005.
- [23] S. Zafar, "Statistical mechanics based model for negative bias temperature instability induced degradation", *J. Appl. Phys.*, vol. 97, no. 10, pp. 1–9, 2005.
- [24] A. Stesmans, "Passivation of  $P_{b0}$  and  $P_{b1}$  interface defects in thermal (100) Si/SiO<sub>2</sub> with molecular hydrogen", *Appl. Phys. Lett.*, vol. 68, no. 15, pp. 2076–2078, 1996.
- [25] M. Houssa, J. L. Autran, A. Stesmans, and M. M. Heyns, "Model for interface defect and positive charge generation in ultrathin SiO<sub>2</sub>/ZrO<sub>2</sub> gate dielectric stacks", *Appl. Phys. Lett.*, vol. 81, no. 4, pp. 709–711, 2002.
- [26] L. Tsetseris, X. J. Zhou, D. M. Fleetwood, R. D. Schrimpf, and S. T. Pantelides, "Physical mechanisms of negative-bias temperature instability", *Appl. Phys. Lett.*, vol. 86, no. 14, pp. 1–3, 2005.
- [27] K. Kushida-Abdelghafar, K. Watanabe, J. Ushio, and E. Murakami, "Effect of nitrogen at SiO<sub>2</sub>/Si interface on reliability issues", *Appl. Phys. Lett.*, vol. 81, no. 23, pp. 4362–4364, 2002.
- [28] M. Houssa, "Modelling negative bias temperature instabilities in advanced p-MOSFETs", *Microelectron. Reliab.*, vol. 45, no. 1, pp. 3–12, 2005.
- [29] N. Stojadinović, D. Danković, S. Djorić-Veljković, V. Davidović, I. Manić, and S. Golubović, "Negative bias temperature instability mechanisms in p-channel power VDMOSFETs", *Microelectron. Reliab.*, vol. 45, no. 9–11, pp. 1343–1348, 2005.
- [30] B. Kaczer, V. Arkhipov, R. Degraeve, N. Collaert, G. Groeseneken, and M. Goodwin, "Disorder-controlled-kinetics model for negative bias temperature instability and its experimental verification", in *Proc. Int. Rel. Phys. Symp.*, San Jose, USA, 2005, pp. 381–387.
- [31] T. Yang, C. Shen, M. F. Li, C. H. Ang, C. X. Zhu, Y.-C. Yeo, G. Samudra, and D.-L. Kwong, "Interface trap passivation effect in NBTI measurement for p-MOSFET with SiON gate dielectric", *IEEE Electron Dev. Lett.*, vol. 26, no. 10, pp. 758–760, 2005.
- [32] D. S. Ang, "Observation of suppressed interface state relaxation under positive gate biasing of the ultrathin oxynitride gate p-MOSFET subjected to negative-bias temperature stressing", *IEEE Electron Dev. Lett.*, vol. 27, no. 5, pp. 412–415, 2006.
- [33] H. Reisinger, O. Blank, W. Heinrigs, A. Mühlhoff, W. Gustin, and C. Schlünder, "Analysis of NBTI degradation- and recovery-behavior based on ultra fast  $V_i$ -measurements", in *Proc. Int. Rel. Phys. Symp.*, San Jose, USA, 2006, pp. 448–453.
- [34] C. G. Van de Walle and B. R. Tuttle, "Microscopic theory of hydrogen in silicon devices", *IEEE Trans. Electron Dev.*, vol. 47, no. 10, pp. 1779–1786, 2000.
- [35] N. H. Nickel, A. Yin, and S. J. Fonash, "Influence of hydrogen and oxygen plasma treatments on grain-boundary defects in polycrystalline silicon", *Appl. Phys. Lett.*, vol. 65, no. 24, pp. 3099–3101, 1994.
- [36] S. N. Rashkeev, D. M. Fleetwood, D. Schrimpf, and S. T. Pantelides, "Dual behavior of H<sup>+</sup> at Si-SiO<sub>2</sub> interfaces: mobility versus trapping", *Appl. Phys. Lett.*, vol. 81, no. 10, pp. 1839–1841, 2002.
- [37] C. G. Van de Walle, P. J. H. Denteneer, Y. Bar-Yam, and S. T. Pantelides, "Theory of hydrogen diffusion and reactions in crystalline silicon", *Phys. Rev. B*, vol. 39, no. 15, pp. 10791–10808, 1989.
- [38] M. Denais, A. Bravaix, V. Huard, C. Parthasarathy, M. Bidaud, G. Ribes, D. Barge, L. Vishnubhotla, B. Tavel, Y. Rey-Tauriac, F. Perrier, N. Revil, F. Arnaud, and P. Stolk, "New hole trapping characterization during NBTI in 65 nm node technology with distinct nitridation processing", in *Proc. Int. Integr. Reliab. Worksh.*, Lake Tahoe, USA, 2004, pp. 121–124.
- [39] D. S. Ang, S. Wang, and C. H. Ling, "Evidence of two distinct degradation mechanisms from temperature dependence of negative bias stressing of the ultrathin gate p-MOSFET", *IEEE Electron Dev. Lett.*, vol. 26, no. 12, pp. 906–908, 2005.
- [40] E. W. Montroll and H. Scher, "Random walks on lattices. IV. Continuous-time walks and influence of absorbing boundaries", *J. Stat. Phys.*, vol. 9, no. 2, pp. 101–135, 1973.
- [41] H. Scher and E. W. Montroll, "Anomalous transit-time dispersion in amorphous solids", *Phys. Rev. B*, vol. 12, no. 6, pp. 2455–2477, 1975.
- [42] J. Noolandi, "Multiple-trapping model of anomalous transit-time dispersion in *a-Se*", *Phys. Rev. B*, vol. 16, no. 10, pp. 4466–4473, 1977.
- [43] V. I. Arkhipov and A. I. Rudenko, "Drift and diffusion in materials with traps", *Phil. Mag. B*, vol. 45, no. 2, pp. 189–207, 1982.
- [44] D. B. Brown and N. S. Saks, "Time dependence of radiation-induced trap formation in metal-oxide-semiconductor devices as a function of oxide thickness and applied field", *J. Appl. Phys.*, vol. 70, no. 7, pp. 3734–3747, 1991.
- [45] J. Orenstein, M. A. Kastner, and V. Vaninov, "Transient photoconductivity and photo-induced optical absorption in amorphous semiconductors", *Phil. Mag. B*, vol. 46, no. 1, pp. 23–62, 1982.
- [46] F. B. McLean and G. A. Ausman, "Simple approximate solution to continuous-time random-walk transport", *Phys. Rev. B*, vol. 15, no. 2, pp. 1052–1061, 1977.
- [47] V. I. Arkhipov, "Trap-controlled and hopping modes of transport and recombination: similarities and differences", in *Proc. Int. Symp. Elect. Insul. Mater.*, Tokyo, Japan, 1995, pp. 271–274.

- [48] J. Noolandi, "Equivalence of multiple-trapping model and time-dependent random walk", *Phys. Rev. B*, vol. 16, no. 10, pp. 4474–4479, 1977.
- [49] F. W. Schmidlin, "Theory of trap-controlled photoconduction", *Phys. Rev. B*, vol. 16, no. 6, pp. 2362–2385, 1977.
- [50] S. Lathi and A. Das, "Seminumerical simulation of dispersive transport in the oxide of metal-oxide semiconductor devices", *J. Appl. Phys.*, vol. 77, no. 8, pp. 3864–3867, 1995.
- [51] N. Talwalkar, A. Das, and J. Vasi, "Dispersive transport of carriers under nonuniform electric field", *J. Appl. Phys.*, vol. 78, no. 7, pp. 4487–4489, 1995.
- [52] W. B. Jackson and C. C. Tsai, "Hydrogen transport in amorphous silicon", *Phys. Rev. B*, vol. 45, no. 12, pp. 6564–6580, 1992.
- [53] K. L. Brower, "Passivation of paramagnetic Si/SiO<sub>2</sub> interface states with molecular hydrogen", *Appl. Phys. Lett.*, vol. 53, no. 6, pp. 508–510, 1988.
- [54] E. Cartier, J. H. Stathis, and D. A. Buchanan, "Passivation and de-passivation of silicon dangling bonds at the Si(111)/SiO<sub>2</sub> interface by atomic hydrogen", *Appl. Phys. Lett.*, vol. 63, no. 11, pp. 1510–1512, 1993.
- [55] E. Cartier and J. H. Stathis, "Hot-electron induced passivation of silicon dangling bonds at the Si(111)/SiO<sub>2</sub> interface", *Appl. Phys. Lett.*, vol. 69, no. 1, pp. 103–105, 1996.
- [56] A. T. Krishnan, S. Chakravarthi, P. Nicollian, V. Reddy, and S. Krishnan, "Negative bias temperature instability mechanism: the role of molecular hydrogen", *Appl. Phys. Lett.*, vol. 88, no. 15, pp. 1–3, 2006.
- [57] A. Stesmans, "Dissociation kinetics of hydrogen-passivated P<sub>b</sub> defects at the (111)Si/SiO<sub>2</sub> interface", *Phys. Rev. B*, vol. 61, no. 12, pp. 8393–8403, 2000.
- [58] M. Denais, V. Huard, C. Parthasarathy, G. Ribes, F. Perrier, D. Roy, and A. Bravaix, "Perspectives on NBTI in advanced technologies: modelling & characterization", in *Proc. ESSDERC Conf.*, Grenoble, France, 2005, pp. 399–402.
- [59] D. L. Griscom, "Diffusion of radiolytic molecular hydrogen as a mechanism for the post-irradiation buildup of interface states in SiO<sub>2</sub>-on-Si structures", *J. Appl. Phys.*, vol. 58, no. 7, pp. 2524–2533, 1985.
- [60] L. Tsetseris and S. T. Pantelides, "Migration, incorporation, and passivation reactions of molecular hydrogen at the Si-SiO<sub>2</sub> interface", *Phys. Rev. B*, vol. 70, no. 24, pp. 1–6, 2004.
- [61] S. Chakravarthi, A. T. Krishnan, V. Reddy, C. F. Machala, and S. Krishnan, "A comprehensive framework for predictive modeling of negative bias temperature instability", in *Proc. Int. Rel. Phys. Symp.*, Phoenix, USA, 2004, pp. 273–282.
- [62] S. Ogawa, M. Shimaya, and N. Shiono, "Interface-trap generation at ultrathin SiO<sub>2</sub> (4 nm–6 nm)-Si interfaces during negative-bias temperature aging", *J. Appl. Phys.*, vol. 77, no. 3, pp. 1137–1148, 1995.
- [63] J. B. Yang, T. P. Chen, S. S. Tan, and L. Chan, "Analytical reaction-diffusion model and the modeling of nitrogen-enhanced negative bias temperature instability", *Appl. Phys. Lett.*, vol. 88, no. 17, pp. 1–3, 2006.
- [64] C. T. Sah, T. H. Ning, and L. L. Tschopp, "The scattering of electrons by surface oxide charges and by lattice vibrations at the silicon-silicon dioxide interface", *Surf. Sci.*, vol. 32, no. 3, pp. 561–575, 1972.
- [65] M. Kondo and H. Tanimoto, "Accurate Coulomb mobility model for MOS inversion layer and its application to NO-oxynitride devices", *IEEE Trans. Electron Dev.*, vol. 48, no. 2, pp. 265–270, 2001.
- [66] M. A. Alam, "NBTI: a simple view of a complex phenomena", in *Proc. Int. Rel. Phys. Symp.*, San Jose, USA, 2006.
- [67] M. Houssa, M. Aoulaiche, J. L. Autran, C. Parthasarathy, N. Revil, and E. Vincent, "Modeling negative bias temperature instabilities in hole channel metal-oxide-semiconductor field effect transistors with ultrathin gate oxide layers", *J. Appl. Phys.*, vol. 95, no. 5, pp. 2786–2791, 2004.
- [68] V. Huard, M. Denais, F. Perrier, N. Revil, C. Parthasarathy, A. Bravaix, and E. Vincent, "A thorough investigation of MOSFETs NBTI degradation", *Microelectron. Reliab.*, vol. 45, no. 1, pp. 83–98, 2005.
- [69] H. Aono, E. Murakami, K. Okuyama, A. Nishida, M. Minami, Y. Ooji, and K. Kubota, "Modeling of NBTI saturation effect and its impact on electric field dependence of the lifetime", *Microelectron. Reliab.*, vol. 45, no. 7–8, pp. 1109–1114, 2005.
- [70] F. Lau, L. Mader, C. Mazure, Ch. Werner, and M. Orłowski, "Model for phosphorus segregation at the silicon-silicon dioxide interface", *Appl. Phys. A*, vol. 49, no. 6, pp. 671–675, 1989.
- [71] H. Kuflluoglu and M. A. Alam, "A geometrical unification of the theories of NBTI and HCI time-exponents and its implications for ultra-scaled planar and surround-gate MOSFETs", in *Proc. Int. Electron Dev. Meet.*, San Francisco, USA, 2004, pp. 113–116.
- [72] C. Schlünder, R. Brederlow, B. Ankele, W. Gustin, K. Goser, and R. Thewes, "Effects of inhomogeneous negative bias temperature stress on p-channel MOSFETs of analog and RF circuits", *Microelectron. Reliab.*, vol. 45, no. 1, pp. 39–46, 2005.
- [73] H. Kuflluoglu and M. A. Alam, "Theory of interface-trap-induced NBTI degradation for reduced cross section MOSFETs", *IEEE Trans. Electron Dev.*, vol. 53, no. 5, pp. 1120–1130, 2006.
- [74] R. E. Stahlbush and E. Cartier, "Interface defect formation in MOSFETs by atomic hydrogen exposure", *IEEE Trans. Nucl. Sci.*, vol. 41, no. 6, pp. 1844–1853, 1994.
- [75] W. D. Eades and R. M. Swanson, "Calculation of surface generation and recombination velocities at the Si-SiO<sub>2</sub> interface", *J. Appl. Phys.*, vol. 58, no. 11, pp. 4267–4276, 1985.



**Tibor Grasser** was born in Vienna, Austria, in 1970. He received the diplomingenieur degree in communications engineering, the Ph.D. degree in technical sciences, and the *venia docendi* in microelectronics from the Technische Universität Wien in 1995, 1999, and 2002, respectively. He is currently employed as an Associate Professor at the Institute for Microelectronics. Since 1997 he has headed the Minimos-NT development group, working on the successor of the highly successful MiniMOS program. He was a visiting research engineer for Hitachi Ltd., Tokyo, Japan, and for the Alpha Development Group, Compaq Computer Corporation, Shrewsbury, USA. In 2003 he was appointed head of the Christian Doppler Laboratory for TCAD in Microelectronics, an industry-funded research group embedded in the Institute for Microelectronics. Doctor Grasser is the co-author or author of nearly 200 articles in scientific books, journals, and conferences proceedings, is the editor of a book on advanced device simulation, a Senior Member of IEEE, and co-chair of SISPAD 2007. His current scientific interests include circuit and device simulation, device modeling and reliability issues.

e-mail: Grasser@iue.tuwien.ac.at

Christian Doppler Laboratory for TCAD  
in Microelectronics  
Institute for Microelectronics, TU Wien  
Gußhausstraße 27-29  
A-1040 Wien, Austria



**Siegfried Selberherr** was born in Klosterneuburg, Austria, in 1955. He received the degree of diplomingenieur in electrical engineering and the doctoral degree in technical sciences from the Technische Universität Wien in 1978 and 1981, respectively. He has been holding the *venia docendi* on computer-aided design

since 1984. Since 1988 he has been the chair Professor of the Institute for Microelectronics. From 1998 to 2005 he served as dean of the Fakultät für Elektrotechnik und Informationstechnik. Professor Selberherr is a Fellow of the IEEE since 1993. His current research interests are modeling and simulation of problems for microelectronics engineering.

e-mail: [Selberherr@iue.tuwien.ac.at](mailto:Selberherr@iue.tuwien.ac.at)  
Institute for Microelectronics, TU Wien  
Gußhausstraße 27–29  
A-1040 Wien, Austria